Inter-limb differences in parameters of aerobic function and local profiles of deoxygenation during double-leg and counterweighted single-leg cycling.

Danilo Iannetta [1], Louis Passfield [1,2], Ahmad Qahtani [1], Martin J MacInnis [1], Juan M Murias [1]

[1] *Faculty of Kinesiology, University of Calgary, Calgary, Canada*

[2] *School of Sport and Exercise Sciences, University of Kent, Canterbury, United Kingdom*

Running head:

Effect of leg-dominance on aerobic exercise capacity.

Corresponding authors:

Dr. Juan M Murias

Assistant Professor,

Faculty of Kinesiology, University of Calgary

KNB 434, 2500 University Drive NW, Calgary, Alberta, Canada, T2N 1N4

+1 (403) 220-7955

jmmurias@ucalgary.ca

ABSTRACT

It is typically assumed that in the context of double-leg cycling, dominant (DOM_{LEG}) and non-dominant ($NDOM_{LEG}$) legs have similar aerobic capacity and that both contribute equally to the whole-body physiological responses. However, there is a paucity of studies that have systematically investigated maximal and submaximal aerobic performance and characterized the profiles of local muscle deoxygenation in relation to leg-dominance. Using counterweighted single-leg cycling, this study explored whether peak O_2 consumption ($\dot{V}O_{2peak}$), maximal lactate steady-state ($MLSS_p$), and profiles of local deoxygenation [HHb] would be different in the DOM_{LEG} compared with the $NDOM_{LEG}$. Twelve participants performed a series of double-leg and counterweighted single-leg DOM_{LEG} and $NDOM_{LEG}$ *i*) ramp-exercise tests, and *ii*) 30-min constant-load trials. $\dot{V}O_{2peak}$ was greater in the DOM_{LEG} than in the $NDOM_{LEG}$ (2.87±0.42 vs 2.70±0.39 $L \cdot min^{-1}$; $P<0.05$). The difference in $\dot{V}O_{2peak}$ persisted even after accounting for lean mass ($P<0.05$). Similarly, $MLSS_p$ was greater in the DOM_{LEG} than in the $NDOM_{LEG}$ (118±31 vs 109±31 W; $P<0.05$). Furthermore, the amplitude of the [HHb] signal during ramp-exercise was larger in the DOM_{LEG} than in the $NDOM_{LEG}$ during both double-leg (26.0±8.4 vs 20.2±8.8 μM; $P<0.05$) and counterweighted single-leg cycling (18.5±7.9 vs 14.9±7.5 μM; $P<0.05$). Additionally, the amplitudes of the [HHb] signal were highly-to-moderately correlated with the mode-specific $\dot{V}O_{2peak}$ values (ranging from 0.91 to 0.54). These findings showed, in a group of young men, that maximal and submaximal aerobic capacities were greater in the DOM_{LEG} than in the $NDOM_{LEG}$, and that superior peripheral adaptations of DOM_{LEG} may underpin these differences.

New and Noteworthy

It is typically assumed that the dominant and non-dominant legs contribute equally to the whole-physiological responses. In this study, we found that the dominant leg achieved greater peak O_2 uptake values, sustained greater power output while preserving whole-body metabolic stability, and showed larger amplitudes of deoxygenation responses. These findings highlight heterogeneous aerobic capacities of the lower-limbs which have important implications when examining whole-body physiological responses.

Key words: dominant; non-dominant; unilateral exercise; muscle deoxygenation; near-infrared spectroscopy.

INTRODUCTION

In humans, one side of the body is usually preferred over the other to execute voluntary motor actions. In the context of double-leg cycling, where both legs are simultaneously involved in the motor task, there is evidence that the dominant-leg (DOM_{LEG}) contributes more to the generated power than the non-dominant-leg ($NDOM_{LEG}$) (12, 62). The magnitude of the reported asymmetries can vary (e.g., ~1-40%) and is dependent on the variable of interest (e.g., power, torque, etc.), pedaling phase, intensity, and cadence (66). Musculoskeletal and motor control deficits of the $NDOM_{LEG}$ are typically acknowledged to underpin these differences (66), despite muscle activation patterns during cycling reportedly being unaffected by leg dominance (10).

Notwithstanding this evidence, exercise physiology studies generally assume that both legs have similar exercise aerobic capacity and that during cycling they equally contribute to the work that is produced, with the characteristics of whole-body physiological responses (e.g., $\dot{V}O_2$) being the summation of homogenous responses that originate from the DOM_{LEG} and $NDOM_{LEG}$. In support of these assumptions, studies assessing parameters of aerobic function of the right and the left legs have showed no inter-limb differences (45, 60). Additionally, even in studies purposely investigating the effect of leg-dominance, $\dot{V}O_{2peak}$ of the DOM_{LEG} was not different from that of the $NDOM_{LEG}$, with or without normalization for lean mass (9, 42, 63). Similarly, no difference in gross efficiency seemed to exist between the DOM_{LEG} and $NDOM_{LEG}$ when exercising at the same absolute intensity (9). However, a caveat of the studies looking at differences between the DOM_{LEG} and $NDOM_{LEG}$ is that they used "unassisted" single-leg cycling modes, which, due to the accentuated engagement of ipsilateral hip flexor muscles, are less efficient and are associated with greater perception of discomfort (1, 8). Thus, localized pain may lead to exercise failure before the attainment of the "true" maximal aerobic power, regardless of leg-dominance. On the contrary, the use of counterweighted single-leg cycling has been reported to reduce the reliance on the hip flexor muscles (18), which facilitates the

tolerability of higher exercise intensity (1, 45). Thus, it is necessary to investigate whether $\dot{V}O_{2peak}$ would differ between the DOM_{LEG} and the $NDOM_{LEG}$ when using counterweighted single-leg cycling exercise.

In the context of single-leg exercise, it is well known that peak aerobic capacity is not limited by cardiac output ($\dot{Q}$), and that there is a greater availability of blood to the exercising (single) leg than during double-leg exercise (16, 36). As a result, the increase in local O_2 delivery ($\dot{Q}_m$) to utilization ($\dot{V}O_{2m}$) ratio (i.e., $\dot{Q}_m/\dot{V}O_{2m}$) reduces the reliance on O_2 extraction (%) at any given intensity and promotes the achievement of greater maximal O_2 flux rates (36, 52, 57). Moreover, when exercise is performed at a similar relative intensity, the net release of lactate from the exercising leg is lower during single- compared with double-leg cycling (36). While these hemodynamic adjustments during single-leg exercise are well established from a systemic perspective (44), they have not been investigated in conjunction with local indices of muscle deoxygenation nor in relation to leg-dominance. Furthermore, although exercise intensity "thresholds" seemingly occur at the same $\dot{V}O_2$ with single- and double-leg cycling (50), it is unknown whether one leg is capable of sustaining greater power outputs than the other while maintaining steady-state metabolic responses during constant-load exercise. Given that mitochondrial capacity exceeds the O_2 delivery capacity during whole-body exercise (7), metabolic stability may be possible at higher relative power outputs with tasks involving a small muscle mass. Collectively, these are important considerations that need to be addressed given that: *i*) local deoxygenation responses (as measured by the near-infrared spectroscopy (NIRS)-derived deoxy-hemoglobin [HHb] signal) have been associated with high local O_2 flux rates (51), and *ii*) whole-body submaximal aerobic performance is a function of the ability of the working muscles to sustain high rates of ATP resynthesis while preserving local metabolic stability (53).

Thus, the purpose of this study was to perform a thorough characterization of the physiological responses in the DOM_{LEG} and $NDOM_{LEG}$ during maximal and submaximal double-leg and

95 counterweighted single-leg cycling while also characterizing local deoxygenation responses. Given that
96 muscle activation patterns are similar between the DOM_{LEG} and $NDOM_{LEG}$ during counterweighted
97 single-leg cycling (10), and that cycling knee-joint forces during this exercise mode are similar to
98 double-leg cycling (5, 18), the use of counterweighted single-leg cycling permitted the examination,
99 under relatively constant neuromuscular conditions, of potential differences in maximal and
100 submaximal aerobic capacity as well as deoxygenation responses between the DOM_{LEG} *vs* $NDOM_{LEG}$
101 and between single-leg *vs* double-leg cycling.

102 **METHODS**

103 *Participants*

104 A group of recreationally-active men (n=12; mean ± SD values: age 30 ± 8 yr; weight 77 ± 11 kg;
105 height 175 ± 8 cm) voluntarily participated in the study. Participants were aware of the risks and
106 benefits of participating in the study, and all signed an informed consent that was approved by the local
107 research ethics board, in compliance with the latest version of the declaration of Helsinki. All
108 participants were nonsmokers, free of any musculoskeletal condition that could limit their maximal
109 exercise exertion, and not undergoing any medical treatment that could alter their cardiovascular
110 responses to exercise.

111 *Procedures*

112 Each participant visited the laboratory on a minimum of ten occasions to complete the following tests:
113 *i*) two double-leg ramp-incremental tests, *ii*) two counterweighted single-leg ramp-incremental tests
114 (one for each leg), and *iii*) six to eight constant-load trials to determine the power output at maximal-
115 lactate steady state ($MLSS_p$) for double-leg and counterweighted single-leg cycling. Each test was
116 separated by at least 48 hours and performed at a similar time of the day in an environmentally
117 controlled laboratory (temperature: 19-20°C; humidity 50-60%). All participants adhered to the

following pre-test instructions: *i*) no vigorous physical activity the day prior to each test, and *ii*) no food or caffeinated beverages for at least 2 and 8 hours, respectively, prior to each test. Participants were blinded to the power output and to the elapsed time during all sessions but received visual feedback on their pedal cadence – which was selected during the first testing session of each condition (i.e., double-leg and counterweighted single-leg) and maintained consistent during the following visits. The position of the handlebar and the seat was recorded during the first visit and kept consistent for the subsequent visits. Additionally, during all experimental conditions participants wore cycling shoes that attached to the pedals.

During each counterweighted single-leg test, the electromagnetically-braked cycle ergometer (Velotron; RacerMate, Seattle, Wa) was fitted with a custom-built pedal that held a 6.84 kg counterweight. During these trials the non-exercising leg was kept in a resting position on a stationary platform. Two familiarization trials with this setup were performed after the two double-leg ramp tests. Before each counterweighted single-leg cycling test, a 4-min double-leg cycling baseline was performed to allow the subsequent normalization of the electromyographic (EMG) signal of the vastus lateralis (see *data analysis* section). Lateral preference was assessed by means of the Waterloo Footedness Questionnaire (17).

Ramp-incremental test. The ramp incremental test consisted of a 4-min baseline cycling stage at 50 W followed by 30 $W \cdot min^{-1}$ and 10-15 $W \cdot min^{-1}$ continuous increments in power output for double-leg and counterweighted single-leg cycling exercise, respectively. The ramp-incremental test was stopped when participants failed to maintain the targeted cadence by 10 rpm for more than ten consecutive seconds despite strong verbal encouragement, or when volitional exhaustion ensued.

Constant-load exercise. A series of constant-load rides were performed to establish $MLSS_p$ (and 10 W above MLSS ($MLSS_{+10}$)) for double-leg and for both the DOM_{LEG} and $NDOM_{LEG}$ during

141 counterweighted single-leg cycling. Each ride was performed for 30 min or to exhaustion, which ever
142 occurred earlier. $MLSS_p$ corresponded to the highest power output that elicited a difference in blood
143 lactate concentration ($[La^-]_b$) between the 10^{th} and the 30^{th} min of exercise ≤ 1 mM (4). The power
144 output for the first double-leg constant-load trial was determined from a mathematical equation
145 developed in our laboratory (28). For counterweighted single-leg cycling, the power output of the first
146 constant-load trial was set at 65% of double-leg $MLSS_p$ because this mode of exercise permits the
147 tolerance of greater workloads per leg than what would be predicted by simply dividing the double-leg
148 $MLSS_p$ by two (8). Regardless of the exercise mode, the resistance for the subsequent constant-load
149 rides was either increased or decreased by 10 W depending on $[La^-]_b$ responses. $[La^-]_b$ was measured
150 during baseline and at regular intervals (i.e., every 5 minutes) after the power output was increased to
151 the predetermined value. At 10^{th} and 30^{th} min, measures of $[La^-]_b$ were taken in triplicate and the
152 average of the two closest was used for subsequent analyses. Double-leg $MLSS_p$ was established before
153 the DOM_{LEG} and $NDOM_{LEG}$ single-leg $MLSS_p$. The first DOM_{LEG} and $NDOM_{LEG}$ counterweighted
154 single-leg trial was randomly assigned. Thereafter, these trials were alternately performed during the
155 subsequent visits.

156 *Data collection*. Gas exchange and ventilatory variables were measured using a metabolic cart (Quark
157 CPET, Cosmed, Rome, Italy). The breath-by-breath system was comprised of a low-dead space turbine
158 and gas analyzers that were calibrated as per manufacturer's recommendation.

159 An impedance cardiography system (Physioflow, Enduro, Manatec Biomedical, Macheren, France)
160 was used to measure $\dot{Q}$ during the ramp-exercise tests. Briefly, the system relies on variations in
161 transthoracic impedance occurring due to the changes in aorta blood volume to compute stroke volume.
162 $\dot{Q}$ ($L \cdot min^{-1}$) is then calculated by multiplying stroke volume by body surface area and heart rate (13).
163 Positioning of the electrodes and system calibration were performed according to manufacturer's
164 instructions. $\dot{Q}$ data were acquired every 10 seconds.

Capillary blood samples were drawn from the finger and immediately analyzed for $[La^-]_b$ (Biosen C-Line, EKF Diagnostics, Barleben, Germany) during ramp-exercise and constant-load trials.

A frequency-domain NIRS system (Oxiplex TS^{TM}, ISS, Champaign, IL) was used in our study to monitor local [HHb] during ramp-exercise. The total-haemoglobin (*tot*[Hb]) signal was also recorded and subsequently used to correct the [HHb] signal for the adipose tissue thickness (see *Data analysis* section). The NIRS probe was composed of eight laser diodes operating at two wavelengths (λ = 690 and 828 nm, four at each wavelengths), which were pulsed in rapid succession, and a photomultiplier tube. The lightweight plastic NIRS probes consisted of two parallel rows of light-emitting fibers and one detector fibre bundle; the source–detector separations for this probe were 2.0, 2.5, 3.0 and 3.5 cm for both wavelengths. The NIRS probe was placed on the belly of the vastus lateralis muscle of the DOM_{LEG} and $NDOM_{LEG}$ (midpoint between the greater trochanter of the femur and the knee joint). The order during the first two double-leg ramp exercise was randomized. Double-sided tape and an elastic bandage were used to secure the probe in place. An optically dense, black vinyl sheet was used to cover the probe to avoid the intrusion of external light. The apparatus was calibrated on each testing day after a warm-up of at least 30 min, as per the manufacturer recommendations. Data were stored online at an output frequency of 2 Hz, and reduced to 1-s bins for all subsequent analyses within the present study. The area of placement was marked and recorded to ensure consistency for the following visits.

A multi-channel surface electromyography system (Delsys Inc, Boston, MA) was used for monitoring EMG at a sampling rate of 1000 Hz. The bipolar surface electrode (41 × 20 × 5 mm) (DE-2.1, Delsys Inc. Boston, MA) was placed on the belly of the vastus lateralis in proximity (longitudinally) of the NIRS probes after the skin area was shaved, abraded, and cleaned to reduce skin impedance. Bi-adhesive and surgical tape were used to secure the electrodes in place. The electrodes were connected to an EMG amplifier which was connected to the acquisition apparatus (Power Lab, ADInstruments,

188 Bella Vista, Australia) linked to a computer software (LabChart 8, ADInstruments, Bella Vista,
189 Australia). Electrodes placement was recorded to ensure consistency between visits.

190 Lower limb lean mass was measured by dual-energy X-ray absorptiometry (Hologic QDR-4500,
191 Hologic, Bedford, MA).

192 *Data analyses*

193 *Ventilatory and gas exchange data*. For each ramp- and constant-power output trial, the breath-by-
194 breath data were edited and aberrant data lying three SD from the local mean were deleted. Thereafter,
195 the $\dot{V}O_2$ data were interpolated on a second-by-second basis. For both double-leg and counterweighted
196 single-leg exercise $\dot{V}O_{2peak}$ corresponded to the highest $\dot{V}O_2$ value computed from a 30-s rolling
197 average. The highest $\dot{V}O_2$ value recorded during the two double-leg ramp-exercise tests corresponded
198 to double-leg $\dot{V}O_{2peak}$. DOM_{LEG} and $NDOM_{LEG}$ $\dot{V}O_{2peak}$ values during counterweighted single-leg
199 cycling were also expressed as ratio of double-leg $\dot{V}O_{2peak}$ (i.e., $\dot{V}O_{2peak}$ *ratio*) (46). The $\dot{V}O_2$ during the
200 constant-load trials at the 15th and 30th minutes were calculated as the average of 2 min of data
201 surrounding the 15th minute (14th – 16th min) and the last two minutes of the 30-min constant-load
202 exercise. The two minutes average of $\dot{V}O_2$ and respiratory exchange ratio were used to calculate gross
203 efficiency (mechanical work/energy expended per minute) (9).

204 During double-leg ramp-exercise, we used a mono-exponential function and nonlinear least-squares
205 regression (34) to compute the $\dot{V}O_2$ functional gain (G_{ramp}):

206 $$\dot{V}O_2\,(t) = \dot{V}O_{2BSL} + \Delta\dot{V}O_{2ss} \cdot (t - \tau'[1 - e^{-t/\tau'}])$$

207 where $\dot{V}O_2\,(t)$ is the value of $\dot{V}O_2$ at any time during the ramp, $\dot{V}O_{2BSL}$ is the baseline ramp value,
208 $\Delta\dot{V}O_{2ss}$ is the increment above $\dot{V}O_{2BSL}$ required for the power output at time *t*, and τ' is the effective
209 time constant of the response. The fitting window was constrained from the onset (t = 0) to the end of

the ramp-exercise. The gain of the response was computed in relation to time but converted to power output and expressed as $\Delta\dot{V}O_2/PO$ ($ml \cdot min^{-1} \cdot W^{-1}$).

Given the well-documented departure from linearity of the $\dot{V}O_2$ response during single-leg ramp-exercise (40, 45), a piecewise equation with two linear segments was used to fit the $\dot{V}O_2$ data as a function of power output and calculate the $\dot{V}O_2$ functional gain in the two regions of ramp-exercise (G_1 and G_2) :

$$f = \text{if } (PO < TD_{PO} \text{ use } g(t), \text{ else } h(t)); \; g(t) = i_1 + s_1 t; \; i_2 = i_1 + s_1 t; \; h(t) = i_2 + s_2 t - TD_{PO}$$

where f is the piecewise function, PO is the power output and g and h are $\dot{V}O_2$, TD_{PO} is the power output corresponding to the intersection of the two regression lines, i_1 and i_2 are the intercepts of the first and second linear function, respectively, and s_1 (i.e., G_1) and s_2 (i.e., G_2) are the slopes with respect to power output ($\Delta\dot{V}O_2/PO$ expressed in $ml \cdot min^{-1} \cdot W^{-1}$).

Cardiac output. $\dot{Q}$ data were edited and aberrant data lying three SD from the local mean were deleted. Thereafter, the $\dot{Q}$ data were interpolated on a second-by-second basis. Baseline $\dot{Q}$ corresponded to last two minutes of baseline before the ramp-onset, whereas $\dot{Q}_{peak}$ corresponded to the highest $\dot{Q}$ computed from a 30-s rolling average. Baseline $\dot{Q}$ values and $\dot{Q}_{peak}$ were used to compute the functional gain with respect to $\dot{V}O_2$ ($\Delta\dot{Q}/\dot{V}O_2$ expressed in $L \cdot min^{-1} \cdot L^{-1(\dot{V}O2)}$).

Adipose tissue thickness correction of [HHb] signals. The [HHb] signal was analyzed after accounting for the adipose tissue thickness under the area of NIRS interrogation (15). Briefly, a Harpenden skin caliper (Baty Int., West Sussex, UK) was used to measure the adipose tissue thickness (mm) in the area of NIRS probe placement. The same investigator took measurements in duplicate and the average of the two was used. Subsequently, a linear regression analysis of the relationship between the adipose tissue thickness and resting *tot*[Hb] was calculated and the measured [HHb] data were corrected to a common adipose tissue thickness of 0 mm (15).

[HHb] during ramp incremental test. The [HHb] data recorded during the ramp-incremental test on the vastus lateralis muscle were plotted against time and modeled with the following segmented piece-wise linear fit, as previously described (67):

$$f = \text{if } (x < BP, g(x), h(x))$$

$$g(x) = i_1 + (s_1 \cdot x)$$

$$i_2 = i_1 + (s_1 \cdot BP)$$

$$h(x) = i_2 + (s_2 \cdot (x - BP))$$

$$\text{fit } f \text{ to } y,$$

where f is the double-linear function, x is time and y is [HHb], BP is the time coordinate corresponding to the interception of the two regression lines (i.e., [HHb] breakpoint), i_1 and i_2 are the intercepts of the first and second linear function, respectively, and s_1 and s_2 are the slopes. Model parameter estimates for each participant were determined by linear least-square regression analysis. A preliminary fit was used to identify and delete aberrant data that were ± 3 SD from the local mean. The model fit was used from the onset of the systematic increase in the [HHb] signal until the last data point corresponding to the end of the test. The power output corresponding to the [HHb] breakpoint was then determined by linear interpolation. Subsequently, the slope of change in the [HHb] signal during ramp-exercise was calculated based on the relative increase in power output (e.g., 0%= baseline; 100= PO_{peak}).

Surface electromyography. The EMG data recorded during the ramp-exercise were amplified, band-pass filtered (5 – 500 Hz), rectified, and computed as 1-s root mean square (RMS) amplitude. Afterwards, regardless of condition, the edited EMG data were normalized to the average of the last two minutes of the baseline double-leg cycling at 50 W and, thereafter, averaged into 10% of peak power output interval-bins for subsequent statistical analysis. The specific normalization strategy was

selected as it is representative of the actual dynamic muscular patterns during cycling. Furthermore, it allowed the comparison of muscle activation between double-leg and counterweighted single-leg cycling exercise.

Statistical Analysis

Data are presented as mean±standard deviation (SD). Repeated-measures ANOVA was performed to detect potential differences in $\dot{V}O_{2peak}$, PO_{peak}, HR_{max}, $\dot{Q}_{peak}$, $\dot{Q}$ gain with respect to $\dot{V}O_2$, peak $[La^-]_b$, [HHb] amplitudes, and [HHb] breakpoints between the different exercise modes during ramp-exercise. Furthermore, repeated-measures ANOVA was performed to detect differences in EMG at 10 % intervals during the ramp-exercise across the different exercise-modes. Pearson's coefficients were calculated to evaluate the level of correlation between the amplitudes of the [HHb] signal and $\dot{V}O_{2peak}$. Student's t-tests were used to compare means values for: *i*) lean mass between DOM_{LEG} and $NDOM_{LEG}$, *ii*) $\dot{V}O_{2peak}$ between the DOM_{LEG} and $NDOM_{LEG}$ normalized for lean mass, *iii*) $\dot{V}O_2$ at the 15^{th} and the 30^{th} min during the constant-load trials. Where appropriate a Bonferroni's *post hoc* analysis was performed. Statistical significance was set at a α level of <0.05.

RESULTS

Ramp exercise

Peak physiological responses to double-leg and counterweighted single-leg ramp-exercise are displayed in Table 1. PO_{peak}, $\dot{V}O_{2peak}$, $\dot{Q}_{peak}$, HR_{max}, and $[La^-]_b$ were higher during double-leg compared with counterweighted single-leg ramp-exercise (*P<0.05*). During counterweighted single-leg ramp exercise, PO_{peak}, $\dot{V}O_{2peak}$, and $\dot{Q}_{peak}$ were 7.5±5.7%, 6.0±5.4%, and 6.2±6.5% higher when exercising with the DOM_{LEG} compared with the $NDOM_{LEG}$, respectively (*P<0.05*). The $\dot{V}O_{2peak}$ *ratio* values for the DOM_{LEG} and $NDOM_{LEG}$ were 0.84±0.05 and 0.79±0.05, respectively. Figure 1 (A,B) depicts the group mean data for $\dot{V}O_2$ and $\dot{Q}$ during ramp-exercise for each exercise mode. There was no difference in the

gain of $\dot{Q}$ with respect to $\dot{V}O_2$ between double-leg and counterweighted single-leg DOM_{LEG} and $NDOM_{LEG}$ ramp-exercise (4.9±0.8, 5.2±1, 5.0±0.9 $L \cdot min^{-1} \cdot L^{-1(\dot{V}O2)}$, respectively; *P>0.05*).

Lower limbs lean mass. No differences in lean mass between the DOM_{LEG} (11.0±1.3 kg) and $NDOM_{LEG}$ (10.8±1.2 kg) were detected (*P>0.05*). There was no significant correlation between lean mass and $\dot{V}O_{2peak}$ of the DOM_{LEG} (r = -0.06, *P>0.05*), nor between lean mass and $\dot{V}O_{2peak}$ of the $NDOM_{LEG}$ (r = 0.32, *P>0.05*). The difference in $\dot{V}O_{2peak}$ between the DOM_{LEG} and $NDOM_{LEG}$ persisted even when $\dot{V}O_{2peak}$ values were normalized by leg-specific lean mass. In this case, the normalized $\dot{V}O_{2peak}$ for the DOM_{LEG} was 0.264±0.052 $mL \cdot g^{-1} \cdot min^{-1}$ whereas for the $NDOM_{LEG}$ was 0.250±0.039 $mL \cdot g^{-1} \cdot min^{-1}$ (% difference = 4.57±6.18%; *P<0.05*).

[HHb] signal. One individual was excluded from the analysis as the quality of his [HHb] signal during ramp-exercise was not satisfactory. Table 2 displays the values for baseline, amplitude and slope of increase of the [HHb] signal. Figure 2 shows the dynamic profiles of [HHb] during ramp-exercise as a function of relative (panels A and B) and absolute (panel C) changes in power output. There was no difference at baseline in the [HHb] signal across the exercise modes (*P>0.05*). However, the [HHb] amplitudes during double-leg and counterweighted single-leg cycling were greater in the DOM_{LEG} compared with the $NDOM_{LEG}$ (*P<0.05*). *S*1 of the [HHb] response was similar between legs across the exercise modes when calculated against relative power output (*P>0.05*). However, when calculated against absolute power output (W), *S*1 was greater during single-leg compared to double-leg (*P<0.05*). There was no difference in *S*2 amongst all conditions (*P>0.05*). The [HHb] breakpoints in the DOM_{LEG} and the $NDOM_{LEG}$ during double-leg cycling were not different in terms of $\%PO_{peak}$ (75±7 vs 70±10 %; *P*>0.05), nor in terms of $\%\dot{V}O_{2peak}$ (83±8 vs 80±9 %; *P*>0.05). Similarly, the [HHb] breakpoints in the DOM_{LEG} and the $NDOM_{LEG}$ during single-leg cycling were not different in terms of $\%PO_{peak}$ (63±10 vs 63±9%; *P*>0.05), nor in terms of $\%\dot{V}O_{2peak}$ (68±10 vs 64±9%; *P*>0.05). However, the [HHb]

breakpoints during counterweighted single-leg cycling occurred at lower fractions of $\dot{V}O_{2peak}$ and PO_{peak} compared with double-leg cycling ($P<0.05$).

Figure 3 (panels A-D) displays the correlation plots between the [HHb] amplitudes and the $\dot{V}O_{2peak}$ among legs and exercise modes. There was a strong correlation between the amplitude of the [HHb] signals of both the DOM_{LEG} and the $NDOM_{LEG}$ during double-leg cycling with double-leg $\dot{V}O_{2peak}$ (DOM_{LEG}: r = 0.86, *P<0.05*; $NDOM_{LEG}$: r = 0.91, *P<0.05*). A significant correlation was also detected between the [HHb] amplitude during counterweighted single-leg cycling of the DOM_{LEG} and the leg-specific $\dot{V}O_{2peak}$ (r = 0.64, *P<0.05*) but not for the [HHb] amplitude during counterweighted single-leg cycling of the $NDOM_{LEG}$ and the leg-specific $\dot{V}O_{2peak}$ (r = 0.54, *P>0.05*).

EMG. The peak RMS at the end of double-leg ramp-exercise was 393±150% for the DOM_{LEG} and 355±161% for the $NDOM_{LEG}$ (*P>0.05*); during counterweighted single-leg cycling the peak RMS were 391±129% and 406±150% for DOM_{LEG} and $NDOM_{LEG}$, respectively (*P>0.05*). There was no difference in EMG between the DOM_{LEG} and the $NDOM_{LEG}$ at peak ramp-exercise (*P>0.05*). Throughout the ramp-exercise, the EMG signal was greater during single- compared with double-leg cycling only within the first 10% of the ramp-exercise (irrespective of leg dominance) (*P<0.05*). Thereafter, no differences were detected between exercise modes nor between legs (*P>0.05*). Figure 4 displays the dynamic profiles of EMG during ramp-exercise between legs and exercise modes.

Constant-load exercise

$\dot{V}O_2$ responses to double-leg and counterweighted single-leg constant-load cycling at $MLSS_p$ and $MLSS_{+10}$ are displayed in Table 3. Figure 5 (panels A-D) displays the group mean data for $\dot{V}O_2$, and $[La^-]_b$ at $MLSS_p$ and $MLSS_{+10}$ for double-leg and counterweighted single-leg cycling.

Double-leg. During double-leg constant-load cycling, time-to-exhaustion at $MLSS_{+10}$ during double-leg was 28.6±4.0 min. $\dot{V}O_2$ stabilized at $MLSS_p$ within the first 15 min and was stable until the end of the

trial (15^{th} min = 2.68±0.25 L·min^{-1}; end-trial = 2.72±0.24 L·min^{-1}; *P>0.05*) but progressively increased at $MLSS_{+10}$ (15^{th} min = 2.78±0.29 L·min^{-1}; end-trial = 2.87±0.28 L·min^{-1}; *P<0.05*). Delta $[La^-]_b$ between 10^{th} and 30^{th} min during $MLSS_p$ and $MLSS_{+10}$ were 0.4±05 and 1.5±0.6 mM (*P<0.05*), respectively.

Counterweighted single-leg constant-load exercise. During counterweighted single-leg cycling, $MLSS_p$ (W) of the DOM_{LEG} was greater than $MLSS_p$ of the $NDOM_{LEG}$ (Table 3). $MLSS_p$ (W) of the DOM_{LEG} and $NDOM_{LEG}$ during counterweighted single-leg cycling were highly correlated to double-leg $MLSS_p$ (r = 0.80 and 0.81, respectively; *P<0.05*). Time-to-exhaustions at $MLSS_{+10}$ during the DOM_{LEG} and the $NDOM_{LEG}$ counterweighted single-leg cycling were 26.8±6.0 and 26.0±7.4 min, respectively. There was no difference in gross efficiency between the DOM_{LEG} (20.0±2.3%) and the $NDOM_{LEG}$ (19.5±1.9%) during their respective $MLSS_p$ (*P>0.05*). $\dot{V}O_2$ of the DOM_{LEG} was stable at $MLSS_p$ (15^{th} min = 2.16±0.25 L·min^{-1}; end-trial = 2.18±0.24 L·min^{-1}; *P>0.05*) but progressively increased at $MLSS_{+10}$ (15^{th} min = 2.29±0.28 L·min^{-1}; end-trial = 2.38±0.32 L·min^{-1}; *P<0.05*). Similarly, $\dot{V}O_2$ of the $NDOM_{LEG}$ was stable at $MLSS_p$ (15^{th} min = 2.07±0.29 L·min^{-1}; end-trial = 2.08±0.31 L·min^{-1}; *P>0.05*) but progressively increased at $MLSS_{+10}$ (15^{th} min = 2.24±0.32 L·min^{-1}; end-trial = 2.33±0.32 L·min^{-1}; *P<0.05*). Delta $[La^-]_b$ of the DOM_{LEG} at $MLSS_p$ and $MLSS_{+10}$ were -0.2±05 and 1.3±0.2 mM, respectively. Delta $[La^-]_b$ of the $NDOM_{LEG}$ at $MLSS_p$ and $MLSS_{+10}$ were -0.2±04 and 1.7±0.9 mM, respectively.

DISCUSSION

The aim of this study was to characterize the physiological responses in the DOM_{LEG} and the $NDOM_{LEG}$ double-leg and counterweighted single-leg cycling in order to gain further insights on the potential mechanisms that determine central and peripheral responses to maximal and submaximal exercise. The main findings were as follows: *i*) during counterweighted single-leg cycling, the DOM_{LEG}

achieved greater $\dot{V}O_{2peak}$ values during ramp-exercise compared with the $NDOM_{LEG}$; *ii*) the DOM_{LEG} was able to sustain greater power outputs compared with the $NDOM_{LEG}$ at an intensity that reflected the critical intensity for counterweighted single-leg exercise; *iii*) during double-leg cycling, the amplitudes of the [HHb] signal for each leg were highly correlated with $\dot{V}O_{2peak}$ and were greater in the DOM_{LEG} compared with the $NDOM_{LEG}$; *iv*) the pattern of increase of the [HHb] signal during counterweighted single-leg resembled that typically observed during double-leg cycling, although the onset of the characteristic plateau in the [HHb] signal occurred at a lower leg-specific percent of $\dot{V}O_{2peak}$ during single-leg compared with double-leg cycling.

DOM_{LEG} vs $NDOM_{LEG}$ during double-leg and counterweighted single-leg cycling.

In contrast to previous observations (9, 42, 63), the present study found that during single-leg cycling the DOM_{LEG} achieved greater PO_{peak} and $\dot{V}O_{2peak}$ values compared with the $NDOM_{LEG}$. In absolute terms, the inter-limb difference in $\dot{V}O_{2peak}$ was ~6% and persisted (~5%) even after the $\dot{V}O_{2peak}$ values were normalized by leg-specific lean mass. This observation is in contrast to previously reported data showing that inter-limb discrepancies in absolute $\dot{V}O_{2peak}$ between the DOM_{LEG} and the $NDOM_{LEG}$ during single-leg cycling were due to differences in lean mass (63). The authors indicated that, in a scenario where $\dot{Q}_m$ is not a limiting factor (36), a greater muscle mass can achieve greater power outputs and, thus, higher absolute metabolic rates (46, 63). However, in the present study, given that differences in $\dot{V}O_{2peak}$ persisted even after normalization for lean mass of the DOM_{LEG} and the $NDOM_{LEG}$, it is likely that other peripheral factors contributed to the observed differences in PO_{peak} and $\dot{V}O_{2peak}$.

From this perspective, we characterized the profiles of the [HHb] signal during double-leg and single-leg ramp exercise in the DOM_{LEG} and the $NDOM_{LEG}$ (Figure 2, A-C). The [HHb] signal represents an index of local fractional O_2 extraction (21), and its amplitude during double-leg incremental-exercise

has been suggested to relate to the capacity of the active muscle fibers to extract O_2 from the surrounding microcirculation and has been found to be positively correlated to $\dot{V}O_{2peak}$ (51). This latter speculation agrees with our findings (Figure 3). Furthermore, we found that the [HHb] amplitudes were greater in the DOM_{LEG} compared with the $NDOM_{LEG}$ during both double- and counterweighted single-leg cycling. In addition to this, we found that the power output and the $\dot{V}O_2$ at MLSS during single-leg cycling were greater in the DOM_{LEG} than in the $NDOM_{LEG}$ (~10 W and ~100 $mL \cdot min^{-1}$, respectively) (Table 3, Figure 5, A and B); interestingly, despite this increased power output and metabolic rate, $[La^-]_b$ values at the respective $MLSS_p$ were similar between the two legs (Figure 5, C and D).

Collectively, these observations support the idea that dissimilar peripheral adaptations may play an important role in the differences in maximal and submaximal aerobic capacity between the DOM_{LEG} and the $NDOM_{LEG}$. Indeed, superior capacity for fractional O_2 extraction and higher metabolic rates at $MLSS_p$ (or similar "thresholds") are both associated with enhanced oxidative capacity (24, 33, 48). However, whether these superior peripheral adaptations in the DOM_{LEG} stem from functional or structural differences is presently unknown. In this perspective, inter-limb "asymmetries" in functional hemodynamics responses, potentially leading to a more efficient diffusion of O_2 at the capillary-to-muscle interface (19, 36), are possible when one limb is regularly exposed to a greater metabolic stress compared with the other limb (59, 64, 65). However, this was likely not the case in the present study, as none of our participants was engaged in unilateral-type activities that would be expected to cause enhanced functional adaptations of the DOM_{LEG}. Interestingly, a recent investigation observed, in a large group of resistance-trained men, that type I fibers were more abundant in the DOM_{LEG} compared with the $NDOM_{LEG}$ (3). Although the biological reasons underpinning these asymmetries in fiber type distribution are elusive at this moment, these observations may support the interpretation of a greater oxidative potential of the DOM_{LEG}. Indeed, type I fibers have a greater oxidative capacity, an increased number of capillaries perfusing each fiber, and a greater $\dot{Q}_m/\dot{V}O_{2m}$ ratio (47, 61), all of which are

important features for the achievement of high O_2 flux rates. This interpretation, however, must be taken with caution as in previous studies fiber type distribution between legs was not different (43, 60).

Alternatively, it could be hypothesized that a superior neuromuscular control of the DOM_{LEG} (e.g., a smaller amount of muscle fibers needed to be recruited to sustain a given power output) would result in a lower ATP requirement to support a given metabolic rate (i.e., improved efficiency). However, we found no difference in the pattern of activation of the vastus lateralis muscle in the $NDOM_{LEG}$ compared to the DOM_{LEG} throughout the counterweighted single-leg (nor double-leg) ramp-exercise (Figure 4). Additionally, no difference in gross efficiency and $\dot{V}O_2$ functional gain (i.e., G_1 and G_2) were found between the DOM_{LEG} and the $NDOM_{LEG}$ when exercising at $MLSS_p$ and during the ramp-exercise, respectively. Thus, considering our findings and those of a previous study which also showed no difference in efficiency between the DOM_{LEG} and the $NDOM_{LEG}$ (9), it is unlikely that a potential enhanced neuromuscular control of the DOM_{LEG} played a major role.

DOM_{LEG} vs $NDOM_{LEG}$: implications for double-leg cycling

There is evidence of marked heterogeneity in the way O_2 is delivered and utilized within the same muscle or muscular groups (30, 41). The present study provides novel information showing not only that the DOM_{LEG} and the $NDOM_{LEG}$ may have different capacities to deliver and utilize O_2 but also that, when tested separately using counterweighted single-leg cycling, they differ in terms of maximal and submaximal aerobic capacity. The question that arises from these observations is, how do these inter-limb differences affect double-leg cycling aerobic performance? In the context of maximal aerobic exercise, given that mitochondrial potential "exceeds" O_2 delivery capacity within the active muscles (7), one possibility is that, even when marked inter-limb differences exist, the "weaker" leg – from an oxidative capacity perspective – may not be a factor limiting whole-body $\dot{V}O_{2peak}$. However, given that O_2 diffusive limitations may exist even in the presence of a reserve in mitochondrial capacity

(56), it could still be possible that the "weakest link" (i.e., the $NDOM_{LEG}$ in the present study) may set the peripheral upper limit for whole body $\dot{V}O_{2peak}$. Additionally, assuming a perfect symmetry in the generated power output between legs, the finding of a lower $MLSS_p$ in the $NDOM_{LEG}$ compared to DOM_{LEG} may imply that during double-leg cycling, the $NDOM_{LEG}$ might contribute more to the progressive loss of whole-body metabolic stability. From this perspective, given that fatigue-sensitive afferent feedback (i.e. group III/IV) from exercising muscles is an important modulator of compensatory (e.g., increase in ventilation (2)) and perceptual responses (26), it is possible that increased feedback from the $NDOM_{LEG}$ may trigger and/or alter these responses earlier or to a greater extent compared to those from the DOM_{LEG} during the task. It is important to acknowledge, however, that the generation of power output during double-leg cycling in "*real life*" scenarios may not be symmetric between legs (11). In this circumstance, a neural strategy that promotes a higher contribution to the generated power output of the leg with the greatest oxidative capacity (e.g., the DOM_{LEG} in the context of the present study) could be hypothesized; this strategy, in line with the *optimal control theory* for motor control (69), could be adopted to *i*) optimize metabolic efficiency, and *ii*) minimize neural drive and perceptual responses (25). However, future studies will be required to test this hypothesis.

Single-leg vs Double-leg; implications for $\dot{V}O_2$ and [HHb] responses

In this study, the $\dot{V}O_2$ response during counterweighted single-leg cycling was consistent with the notion that above the critical intensity of exercise (in this case represented by MLSS), attainment of $\dot{V}O_2$ steady-state is no longer feasible (55). It is interesting to note, however, that during counterweighted single-leg cycling, the "upper limit" at which $\dot{V}O_2$ steady-state was attainable represented ~80% of the $\dot{V}O_2$ corresponding to the double-leg $MLSS_p$. The augmented capacity of the (single) exercising leg to sustain work in steady-state condition at a greater metabolic rate compared to double-leg is likely due to the increase in O_2 availability during single-leg exercise. Indeed, an

441 increased O_2 availability enhances the "critical metabolic rate" at which oxidative phosphorylation is
442 able to provide all the ATP required by the task (70). In the context of double-leg cycling, this implies
443 that, at any submaximal power output, increasing local O_2 delivery (by convection or diffusion) will
444 reduce the reliance on substrate level phosphorylation and the magnitude of the $\dot{V}O_2$ slow component,
445 with this mechanisms having important implications for the etiology of fatigue and exercise tolerance
446 (22, 35).

447 In agreement with previous reports using single-leg models (either knee-extension (57) or cycling
448 ergometers (38, 45)), the slope of the $\dot{V}O_2$-to-power output relationship during ramp-exercise was
449 greater and "upwardly-curvilinear" during single-leg compared to double-leg cycling (Figure 1, A). In
450 the context of the present study, there are several putative reasons that might have contributed to the
451 greater and progressively increasing $\dot{V}O_2$ cost for a given change in power output during
452 counterweighted single-leg compared to double-leg ramp-exercise: *i*) earlier/greater activation of type
453 II fibers (36) which might necessitate a greater O_2 cost of contraction; *ii*) disproportional increase of
454 $\dot{V}O_2$ associated with ventilatory and postural muscle activity (16, 54); *iii*) slower rate of increase in
455 power output during single-leg (15-20 $W \cdot min^{-1}$) *vs* double-leg ramp-exercise, which allowed more time
456 for muscle $\dot{V}O_2$ kinetics to be developed and expressed at the level of the mouth (27, 71); *iv*) greater
457 and progressively increasing external forces associated with the counterweight load applied on the
458 contralateral crank, which might increase the O_2 cost of pedaling at a given power output. Although
459 discriminating among these factors would require uniform exercise protocols between double- and
460 single-leg exercise (i.e., similar ramp-rate) as well as continuous measurements of leg blood flow, $\dot{V}O_2$,
461 and EMG, the analysis of the [HHb] patterns from the present study offers some insights. We found
462 that the s*lope 1* of the [HHb] signal during ramp-exercise was unchanged between counterweighted
463 single-leg and double-leg cycling when normalized to the relative power output (Figure 2; Table 2).
464 This observation could imply that the balance between O_2 delivery and utilization remained unaltered

between the two exercise modes, which is partly confirmed by the similar patterns of increase in EMG between single- *vs* double-leg cycling (Figure 4). It must be acknowledged, however, that a greater mass-specific blood flow during counterweighted single-leg exercise might have promoted a greater $\dot{Q}_m/\dot{V}O_{2m}$ ratio (39), confounding the interpretation of the dynamic changes of the [HHb] signal across different exercise modes. However, the relationship between $\dot{Q}_m$ and $\dot{V}O_{2m}$ during single-leg exercise could be have been preserved considering that the greater mass-specific blood flow could be matched with the greater mass-specific metabolic rate associated with single-leg exercise (38). Overall, these adjustments may have preserved the same dynamics between O_2 delivery and utilization during single-leg exercise. This suggestion finds support in the observation that, similarly to the $\dot{V}O_2$ response, at a given power output there was a greater [HHb] signal during single-leg cycling compared to double-leg cycling (Figure 2, C). Collectively, these observations may justify the hypothesis that the greater O_2 cost of counterweighted single-leg cycling may primarily originate within the working musculature of the exercising leg, although some contribution of areas outside of the exercising muscles cannot be excluded (54).

The observation of a plateau in the [HHb] signal during counterweighted single-leg exercise is interesting and may help shed light on the debated physiological mechanisms underpinning this phenomenon (6, 20, 29, 32). In this regard, it has been suggested that the plateau in the [HHb] signal during ramp-incremental cycling is explained by a greater $Q_m/\dot{V}O_{2m}$ in the region of NIRS interrogation driven by locally-released vasodilators at metabolic rates similar to, or above, the maximal lactate steady state (49). This redistribution of blood flow would happen at the expenses of less metabolically challenged areas of the quadriceps muscles, and be dictated by the fiber type characteristics of the region investigated (14, 68). Contrarily, it was recently suggested that the levelling-off of the [HHb] signal during double-leg ramp-exercise is caused by the lower O_2 diffusion gradient due to the near-equilibrium between the microvascular and intramyocyte O_2 pressures that is

achieved at near-maximal exercise intensities (20). However, if this suggestion were true, a plateau in the [HHb] response should have not occurred during single-leg cycling, as the greater microvascular O_2 pressure resulting from the greater mass-specific blood flow (37, 57) should have preserved the O_2 diffusion gradient up to near-maximal intensities, thus allowing the [HHb] to continue its increase until exercise termination (i.e., $\dot{V}O_{2peak}$). Yet, the [HHb] signal during counterweighted single-leg plateaued at even slightly lower percentages of leg-specific $\dot{V}O_{2peak}$ compared to double-leg cycling (Figure 2). Therefore, while recognizing that a reduced O_2 diffusion gradient will eventually limit the achievement of higher O_2 flux rates at maximal exercise intensity (particularly during double-leg exercise) (58), the present data question whether this mechanism would underpin the [HHb] plateau.

Methodological considerations

An important methodological difference compared with previous studies examining maximal aerobic capacity of the DOM_{LEG} and the $NDOM_{LEG}$ (9, 42, 63) is that in the present study the exercising leg during single-leg cycling was assisted by a weight applied to the contralateral crank. This setup, by reducing the discomfort associated with the excessive engagement of the ipsilateral hip flexor muscles during the upstroke phase (8), might have facilitated the achievement of leg-specific aerobic performance that was closer to the "true" maximum for the limb under investigation. This suggestion is supported by the fact that the average $\dot{V}O_{2peak}$ *ratio* (i.e., the ratio between single-leg and double-leg $\dot{V}O_{2peak}$) was 0.84 for the DOM_{LEG}, while in a previous investigation using "unassisted" single-leg cycling this ratio was 0.76 (46). Therefore, recognizing that inter-limb asymmetries in maximal and submaximal aerobic capacity might be subtle (63), the use of a counterweight may be important for their detection.

Furthermore, it is important to consider that the application of the counterweight reduces but does not abolish biomechanical differences between single- *vs* double-leg cycling (18). Therefore, although we

assume similar neuromuscular dynamics between these two exercise modes, potential differences in joint kinematics (which could also be expressed differently in relation to limb dominance) could have played a role in our findings. This is an important methodological consideration for the interpretation of our results, where the [HHb] signal is tightly matched to the level of muscle activity and resultant dynamics of local blood flow (31, 39).

Finally, in this study the [HHb] response of the vastus lateralis of the quadriceps was monitored, thus our interpretations related to the amplitudes of this signal are specific to that muscle area. However, given that this muscle is the prime mover (23) during cycling and that the relationship between the [HHb] amplitudes and $\dot{V}O_{2peak}$ was observed in other muscle areas of the same muscle group (such as the rectus femoris) (51), it can be suggested that the amplitudes of the [HHb] signal in the vastus lateralis may well reflect the "whole-quadriceps" fractional O_2 extraction capacity.

CONCLUSIONS

To summarize, findings from the present study showed that, during single-leg exercise, the DOM_{LEG} achieved greater $\dot{V}O_{2peak}$ values and was able to sustain greater power outputs with stable metabolic responses compared with the $NDOM_{LEG}$. While the exact physiological reasons of these differences are difficult to establish, the facts that the [HHb] amplitudes and the $MLSS_p$ were greater in the DOM_{LEG} may suggest the presence of superior peripheral adaptations in this leg compared with the $NDOM_{LEG}$. These findings have important implications for the design of future studies using counterweighted single-leg cycling. In addition to this, the present study observed that the patterns of increase of the [HHb] signal during counterweighted single-leg were similar to double-leg cycling during the ramp-exercise. This is indicative of similar dynamics during counterweight single-leg and double-leg cycling in the balance between O_2 delivery and utilization.

ACKNOWLEDGMENTS

We express our gratitude to the participants in this study. We also extend our gratitude to Rafael Azevedo for his help during data collection.

GRANTS

This study was supported by National Science and Engineering Research Council of Canada (RGPIN-2016-03698) and the Heart & Stroke Foundation of Canada (1047725).

DISCLOSURES

The authors declare no conflict of interest

AUTHOR CONTRIBUTIONS

DI, LP, AQ, MJM and JMM conceived and designed research; DI and AQ performed experiments; DI analyzed data; DI, LP, MJM, and JMM interpreted results of experiments; DI prepared figures and drafted the manuscript; DI, LP, AQ, MJM, and JMM edited, revised, and approved final version of manuscript.

REFERENCES

1. **Abbiss CR**, **Karagounis LG**, **Laursen PB**, **Peiffer JJ**, **Martin DT**, **Hawley JA**, **Fatehee NN**, **Martin JC**. Single-leg cycle training is superior to double-leg cycling in improving the oxidative potential and metabolic profile of trained skeletal muscle. *J Appl Physiol* 110: 1248–1255, 2011.

2. **Amann M**, **Blain GM**, **Proctor LT**, **Sebranek JJ**, **Pegelow DF**, **Dempsey JA**. Group III and IV muscle afferents contribute to ventilatory and cardiovascular response to rhythmic exercise in humans. *J Appl Physiol* 109: 966–76, 2010.

3. **Arevalo JA**, **Lynn SK**, **Bagley JR**, **Brown LE**, **Costa PB**, **Galpin AJ**. Lower-Limb Dominance, Performance, and Fiber Type in Resistance-trained Men. *Med Sci Sports Exerc* 50: 1054–1060, 2018.

4. **Beneke R**. Maximal lactate steady state concentration (MLSS): experimental and modelling approaches. *Eur J Appl Physiol* 88: 361–9, 2003.

5. **Bini RR**, **Jacques TC**, **Vaz MA**. Joint Torques and Patellofemoral Force during Single-Leg Assisted and Unassisted Cycling. *J Sport Rehabil* 25: 40–47, 2014.

6. **Boone J**, **Vandekerckhove K**, **Coomans I**, **Prieur F**, **Bourgois JG**. An integrated view on the oxygenation responses to incremental exercise at the brain, the locomotor and respiratory muscles. *Eur J Appl Physiol* 116: 2085–2102, 2016.

7. **Boushel R**, **Gnaiger E**, **Larsen FJ**, **Helge JW**, **González-Alonso J**, **Ara I**, **Munch-Andersen T**, **van Hall G**, **Søndergaard H**, **Saltin B**, **Calbet JAL**. Maintained peak leg and pulmonary VO2despite substantial reduction in muscle mitochondrial capacity. *Scand J Med Sci Sport* 25: 135–143, 2015.

8. **Burns KJ**, **Pollock BS**, **Lascola P**, **McDaniel J**. Cardiovascular responses to counterweighted single-leg cycling: Implications for rehabilitation. *Eur J Appl Physiol* 114: 961–968, 2014.

9. **Carpes FP**, **Diefenthaeler F**, **Bini RR**, **Stefanyshyn D**, **Faria IE**, **Mota CB**. Does leg preference affect muscle activation and efficiency? *J Electromyogr Kinesiol* 20: 1230–1236, 2010.

10. **Carpes FP**, **Diefenthaeler F**, **Bini RR**, **Stefanyshyn DJ**, **Faria IE**, **Mota CB**. Influence of leg preference on bilateral muscle activation during cycling. *J Sports Sci* 29: 151–159, 2011.

11. **Carpes FP**, **Mota CB**, **Faria IE**. On the bilateral asymmetry during running and cycling - A review considering leg preference. *Phys Ther Sport* 11: 136–142, 2010.

12. **Carpes FP**, **Rossato M**, **Faria IE**, **Mota CB**. Bilateral pedaling asymmetry during a simulated 40-km cycling time-trial. *J Sports Med Phys Fitness* 47: 51–57, 2007.

13. **Charloux A**, **Lonsdorfer-Wolf E**, **Richard R**, **Lampert E**, **Oswald-Mammosser M**, **Mettauer B**, **Geny B**, **Lonsdorfer J**. A new impedance cardiograph device for the non-invasive evaluation of cardiac output at rest and during exercise: Comparison with the ″direct″ Fick method. *Eur J Appl Physiol* 82: 313–320, 2000.

14. **Copp SW**, **Hirai DM**, **Musch TI**, **Poole DC**. Critical speed in the rat: implications for hindlimb muscle blood flow distribution and fibre recruitment. *J Physiol* 588: 5077–87, 2010.

15. **Craig JC**, **Broxterman RM**, **Wilcox SL**, **Chen C**, **Barstow TJ**. Effect of adipose tissue thickness, muscle site, and sex on near-infrared spectroscopy derived total-[hemoglobin + myoglobin]. *J. Appl. Physiol.* .

16. **Davies CT**, **Sargeant AJ**. Physiological responses to one- and two-leg exercise breathing air and 45 percent oxygen. *J Appl Physiol* 36: 142–148, 1974.

17. **Elias LJ**, **Bryden MP**, **Bulman-Fleming MB**. Footedness is a better predictor than is handedness of emotional lateralization. *Neuropsychologia* 36: 37–43, 1998.

18. **Elmer SJ**, **McDaniel J**, **Martin JC**. Biomechanics of counterweighted one-legged cycling. *J Appl Biomech* 32: 78–85, 2016.

19. **Esposito F**, **Reese V**, **Shabetai R**, **Wagner PD**, **Richardson RS**. Isolated quadriceps training increases maximal exercise capacity in chronic heart failure: The role of skeletal muscle convective and diffusive oxygen transport. *J Am Coll Cardiol* 58: 1353–1362, 2011.

20. **Grassi B**. New data and well-established concepts. *J Appl Physiol* 125: 1354–1355, 2018.

21. **Grassi B**, **Pogliaghi S**, **Rampichini S**, **Quaresima V**, **Ferrari M**, **Marconi C**, **Cerretelli P**. Muscle oxygenation and pulmonary gas exchange kinetics during cycling exercise on-transitions in humans. *J Appl Physiol* 95: 149–158, 2015.

22. **Grassi B**, **Rossiter HB**, **Zoladz J a.** Skeletal Muscle Fatigue and Decreased Efficiency. *Exerc Sport Sci Rev* 43: 75–83, 2015.

23. **Hautier CA**, **Arsac LM**, **Deghdegh K**, **Souquet J**, **Belli A**, **Lacour JR**. Influence of fatigue on EMG/force ratio and cocontraction in cycling. *Med Sci Sports Exerc* 32: 839–43, 2000.

24. **Hoppeler H**, **Howald H**, **Conley K**, **Lindstedt SL**, **Claassen H**, **Vock P**, **Weibel ER**. Endurance training in humans: aerobic capacity and structure of skeletal muscle. *J Appl Physiol* 59: 320–327, 1985.

25. **Hug F**, **Goupille C**, **Baum D**, **Raiteri BJ**, **Hodges PW**, **Tucker K**. Nature of the coupling between neural drive and force-generating capacity in the human quadriceps muscle. *Proc R Soc B Biol Sci* 282, 2015.

26. **Hureau TJ**, **Romer LM**, **Amann M**. The “sensory tolerance limit”: A hypothetical construct

613 determining exercise performance? *Eur J Sport Sci* 18: 13–24, 2018.

614 27. **Iannetta D**, **Azevedo R de A**, **Keir DA**, **Murias JM**. Establishing the V̇O 2 versus constant-
615 work rate relationship from ramp-incremental exercise: Simple strategies for an unsolved
616 problem. *J Appl Physiol* 1: japplphysiol.00508.2019, 2019.

617 28. **Iannetta D**, **Fontana FY**, **Maturana FM**, **Inglis EC**, **Pogliaghi S**, **Keir DA**, **Murias JM**. An
618 equation to predict the maximal lactate steady state from ramp-incremental exercise test data in
619 cycling. *J Sci Med Sport* 21: 1274–1280, 2018.

620 29. **Iannetta D**, **Okushima D**, **Inglis EC**, **Kondo N**, **Murias JM**, **Koga S**. Blood flow occlusion-
621 related O 2 extraction "reserve" is present in different muscles of the quadriceps but greater in
622 deeper regions after ramp-incremental test. *J Appl Physiol* 125: 313–319, 2018.

623 30. **Iannetta D**, **Qahtani A**, **Mattioni Maturana F**, **Murias JM**. The near-infrared spectroscopy-
624 derived deoxygenated haemoglobin breaking-point is a repeatable measure that demarcates
625 exercise intensity domains. *J Sci Med Sport* 20: 873–877, 2017.

626 31. **Iannetta D**, **Qahtani A**, **Millet GY**, **Murias JM**. Quadriceps Muscles O2 Extraction and EMG
627 Breakpoints during a Ramp Incremental Test. *Front Physiol* 8: 1–9, 2017.

628 32. **Inglis EC**, **Iannetta D**, **Murias JM**. The plateau in the NIRS-derived [HHb] signal near the end
629 of a ramp incremental test does not indicate the upper limit of O 2 extraction in the vastus
630 lateralis. *Am J Physiol Integr Comp Physiol* 313: R723–R729, 2017.

631 33. **Ivy JL**, **Withers RT**, **Van Handel PJ**, **Elger DH**, **Costill DL**. Muscle respiratory capacity and
632 fiber type as determinants of the lactate threshold. *J Appl Physiol* 48: 523–527, 2017.

633 34. **Keir DA**, **Benson AP**, **Love LK**, **Robertson TC**, **Rossiter HB**, **Kowalchuk JM**. Influence of
634 muscle metabolic heterogeneity in determining the V̇O2p kinetic response to ramp-incremental

exercise. *J Appl Physiol* 120: 503–13, 2016.

35. **Keir DA**, **Copithorne DB**, **Hodgson MD**, **Pogliaghi S**, **Rice CL**, **Kowalchuk JM**. The slow component of pulmonary O 2 uptake accompanies peripheral muscle fatigue during high-intensity exercise. *J Appl Physiol* 121: 493–502, 2016.

36. **Klausen K**, **Secher NH**, **Clausen JP**, **Hartling O**, **Trap-Jensen J**. Central and regional circulatory adaptations to one-leg training. *J Appl Physiol* 52: 976–983, 1982.

37. **Knight DR**, **Schaffartzik W**, **Poole DC**, **Hogan MC**, **Bebout DE**, **Wagner PD**. Effects of hyperoxia on maximal leg O2 supply and utilization in men. *J Appl Physiol* 75: 2586–2594, 1993.

38. **Koga S**, **Barstow TJ**, **Shiojiri T**, **Takaishi T**, **Fukuba Y**, **Kondo N**, **Shibasaki M**, **Poole DC**. Effect of muscle mass on VO2 kinetics at the onset of work. *J Appl Physiol* 90: 461–8, 2001.

39. **Koga S**, **Okushima D**, **Poole DC**, **Rossiter HB**, **Kondo N**, **Barstow TJ**. Unaltered V̇o2 kinetics despite greater muscle oxygenation during heavy-intensity two-legged knee extension versus cycle exercise in humans. *Am J Physiol Regul Integr Comp Physiol* 317: R203–R213, 2019.

40. **Koga S**, **Poole DC**, **Shiojiri T**, **Kondo N**, **Fukuba Y**, **Miura A**, **Barstow TJ**. Comparison of oxygen uptake kinetics during knee extension and cycle exercise. *Am J Physiol Integr Comp Physiol* 288: R212–R220, 2004.

41. **Koga S**, **Rossiter HB**, **Heinonen I**, **Musch TI**, **Poole DC**. Dynamic heterogeneity of exercising muscle blood flow and O2 utilization. *Med Sci Sports Exerc* 46: 860–876, 2014.

42. **Larson RD**, **McCully KK**, **Larson DJ**, **Pryor WM**, **White LJ**. Bilateral differences in lower-limb performance in individuals with multiple sclerosis. *J Rehabil Res Dev* 50: 215–221, 2013.

43. **Lexell J**, **Taylor CC**. A morphometrical comparison of right and left whole human vastus

lateralis muscle: how to reduce sampling errors in biopsy techniques. *Clin Physiol* 11: 271–276, 1991.

44. **MacInnis MJ**, **McGlory C**, **Gibala MJ**, **Phillips SM**. Investigating human skeletal muscle physiology with unilateral exercise models: when one limb is more powerful than two. *Appl Physiol Nutr Metab* 42: 563–570, 2017.

45. **MacInnis MJ**, **Morris N**, **Sonne MW**, **Zuniga AF**, **Keir PJ**, **Potvin JR**, **Gibala MJ**. Physiological responses to incremental, interval, and continuous counterweighted single-leg and double-leg cycling at the same relative intensities. *Eur J Appl Physiol* 117: 1423–1435, 2017.

46. **McPhee JS**, **Williams AG**, **Stewart C**, **Baar K**, **Schindler JP**, **Aldred S**, **Maffulli N**, **Sargeant AJ**, **Jones DA**. The training stimulus experienced by the leg muscles during cycling in humans. *Exp Physiol* 94: 684–694, 2009.

47. **Mitchell EA**, **Martin NRW**, **Bailey SJ**, **Ferguson RA**. Critical power is positively related to skeletal muscle capillarity and type I muscle fibers in endurance-trained individuals. *J Appl Physiol* 125: 737–745, 2018.

48. **Murias JM**, **Kowalchuk JM**, **Paterson DH**. Time course and mechanisms of adaptations in cardiorespiratory fitness with endurance training in older and young men. *J Appl Physiol (Bethesda, Md 1985)* 108: 621–627, 2010.

49. **Murias JM**, **Spencer MD**, **Keir D a**, **Paterson DH**. Systemic and vastus lateralis muscle blood flow and O2 extraction during ramp incremental cycle exercise. *AJP Regul Integr Comp Physiol* 304: 720–725, 2013.

50. **Neary PJ**, **Wenger HA**. The effects of one- and two-legged exercise on the lactate and ventilatory threshold. *Eur J Appl Physiol Occup Physiol* 54: 591–595, 2005.

679 51. **Okushima D**, **Poole DC**, **Barstow TJ**, **Rossiter HB**, **Kondo N**, **Bowen TS**, **Amano T**, **Koga S**.
680 Greater VO2peak is correlated with greater skeletal muscle deoxygenation amplitude and
681 hemoglobin concentration within individual muscles during ramp-incremental cycle exercise.
682 *Physiol Rep* 4: 1–12, 2016.

683 52. **Pernow B**, **Saltin B**. Availability of substrates and capacity for prolonged heavy exercise in
684 man. *J Appl Physiol* 31: 416–422, 1971.

685 53. **Poole DC**, **Burnley M**, **Vanhatalo A**, **Rossiter HB**, **Jones AM**. Critical power: An important
686 fatigue threshold in exercise physiology. *Med Sci Sports Exerc* 48: 2320–2334, 2016.

687 54. **Poole DC**, **Richardson RS**. Determinants of oxygen uptake: Implications for exercise testing.
688 *Sport Med* 24: 308–320, 1997.

689 55. **Poole DC**, **Ward SA**, **Gardner GW**, **Whipp BJ**. Metabolic and respiratory profile of the upper
690 limit for prolonged exercise in man. *Ergonomics* 31: 1265–79, 1988.

691 56. **Richardson RS**, **Knight DR**, **Poole DC**, **Kurdak SS**, **Hogan MC**, **Grassi B**, **Wagner PD**.
692 Determinants of maximal exercise VO2 during single leg knee-extensor exercise in humans. *Am*
693 *J Physiol* 268: H1453-61, 1995.

694 57. **Richardson RS**, **Poole DC**, **Knight DR**, **Kurdak SS**, **Hogan MC**, **Grassi B**, **Johnson EC**,
695 **Kendrick KF**, **Erickson BK**, **Wagner PD**. High muscle blood flow in man: is maximal O2
696 extraction compromised? *J Appl Physiol* 75: 1911–1916, 1993.

697 58. **Roca J**, **Hogan MC**, **Story D**, **Bebout DE**, **Haab P**, **Gonzalez R**, **Ueno O**, **Wagner PD**.
698 Evidence for tissue diffusion limitation of VO2max in normal humans. *J Appl Physiol* 67: 291–
699 299, 1989.

700 59. **Rowley NJ**, **Dawson EA**, **Birk GK**, **Cable NT**, **George K**, **Whyte G**, **Thijssen DHJ**, **Green**

DJ. Exercise and arterial adaptation in humans: Uncoupling localized and systemic effects. *J Appl Physiol* 110: 1190–1195, 2011.

60. **Saltin B**, **Costill DL**, **Essén B**, **Jansson E**, **Gollnick PD**, **Nazar K**, **Stein E**. The Nature of the Training Response; Peripheral and Central Adaptations to One-Legged Exercise. *Acta Physiol Scand* 96: 289–305, 2008.

61. **Saltin B**, **Henriksson J**, **Nygaard E**, **Andersen P**, **Jansson E**. Fiber Types and Metabolic Potentials of Skeletal Muscles in Sedentary Man and Endurance Runners. *Ann N Y Acad Sci* 301: 3–29, 1977.

62. **Sargeant AJ**, **Davies CT**. Forces applied to cranks of a bicycle ergometer during one- and two-leg cycling. *J Appl Physiol* 42: 514–518, 1977.

63. **Sargeant AJ**, **Davies CTM**. Limb volume, composition, and maximum aerobic power output in relation to habitual "preference" in young male subjects. *Ann Hum Biol* 4: 49–55, 1977.

64. **Sinoway LI**, **Musch TI**, **Minotti JR**, **Zelis R**. Enhanced maximal metabolic vasodilatation in the dominant forearms of tennis players. *J Appl Physiol* 61: 673–678, 1986.

65. **Sinoway LI**, **Shenberger J**, **Wilson J**, **McLaughlin D**, **Musch T**, **Zelis R**. A 30-day forearm work protocol increases maximal forearm blood flow. *J Appl Physiol* 62: 1063–1067, 2017.

66. **Smak W**, **Neptune RR**, **Hull ML**. The influence of pedaling rate on bilateral asymmetry in cycling. *J Biomech* 32: 899–906, 1999.

67. **Spencer MD**, **Murias JM**, **Paterson DH**. Characterizing the profile of muscle deoxygenation during ramp incremental exercise in young men. *Eur J Appl Physiol* 112: 3349–3360, 2012.

68. **Thomas GD**, **Hansen J**, **Victor RG**. Inhibition of alpha 2-adrenergic vasoconstriction during contraction of glycolytic, not oxidative, rat hindlimb muscle. *Am J Physiol Circ Physiol* 266:

723 H920–H929, 1994.

724 69. **Todorov E**. Optimality principles in sensorimotor control. *Nat Neurosci* 7: 907–915, 2004.

725 70. **Vanhatalo A**, **Fulford J**, **Dimenna FJ**, **Jones AM**. Influence of hyperoxia on muscle metabolic
726 responses and the power-duration relationship during severe-intensity exercise in humans: A 31P
727 magnetic resonance spectroscopy study. *Exp Physiol* 95: 528–540, 2010.

728 71. **Wilcox SL**, **Broxterman RM**, **Barstow TJ**. Constructing quasi-linear V̇O2 responses from
729 nonlinear parameters. *J Appl Physiol* 120: 121–9, 2016.

730

FIGURE CAPTIONS

Figure 1. Group mean data of $\dot{V}O_2$ ($L \cdot min^{-1}$) and $\dot{Q}$ ($L \cdot min^{-1}$) with respect to absolute power output during double-leg and counterweighted single-leg cycling. * Denotes significance between counterweighted single-leg and double-leg cycling. # Denotes significance between dominant (DOM_{LEG}) and non-dominant ($NDOM_{LEG}$).

Figure 2. Group mean [HHb] (μM) profiles with respect to relative (A,B) and absolute (C) power output during double-leg and counterweighted single-leg cycling. * Denotes significance in relation to [HHb] signal amplitude between dominant (DOM_{LEG}) and non-dominant ($NDOM_{LEG}$). # Denotes significance in relation to *slope 1* of the [HHb] signal between counterweighted single- *vs* double-leg cycling (irrespective of leg-dominance). For clarity, *y*-axis error bars on panel C are not displayed.

Figure 3. Relationship between the amplitude of the [HHb] (μM) signal and $\dot{V}O_{2max}$ ($L \cdot min^{-1}$) recorder at the end of double-leg and counterweighted single-leg ramp-exercise in the DOM_{LEG} and $NDOM_{LEG}$. * <0.05.

Figure 4. Group mean EMG profiles (%RMS) with respect to relative power output during double-leg and counterweighted single-leg ramp-exercise in the DOM_{LEG} and $NDOM_{LEG}$. * Denotes significance at the corresponding time-point between counterweighted single- *vs* double-leg cycling (irrespective of leg-dominance).

Figure 5. Group mean data of $\dot{V}O_2$ ($L \cdot min^{-1}$) and $[La^-]_b$ (μM) during double-leg and DOM_{LEG} and $NDOM_{LEG}$ counterweighted single-leg cycling at $MLSS_p$ and $MLSS_{+10}$. Refer to the Results section for loci of significance.

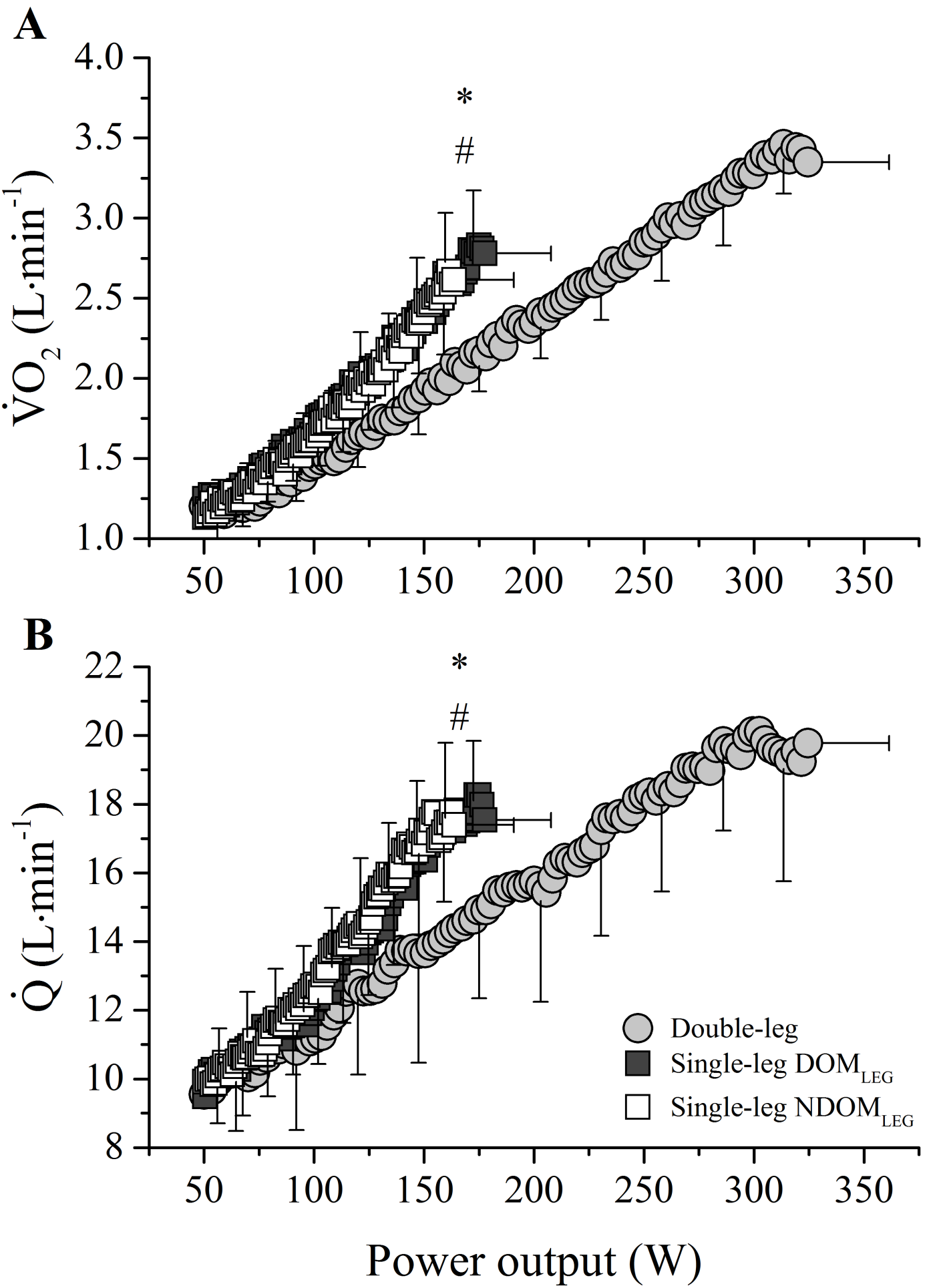
A
B
$\dot{V}O_2$ (L·min^{-1})
$\dot{Q}$ (L·min^{-1})
*
#
Double-leg
Single-leg DOM$_{LEG}$
Single-leg NDOM$_{LEG}$
Power output (W)

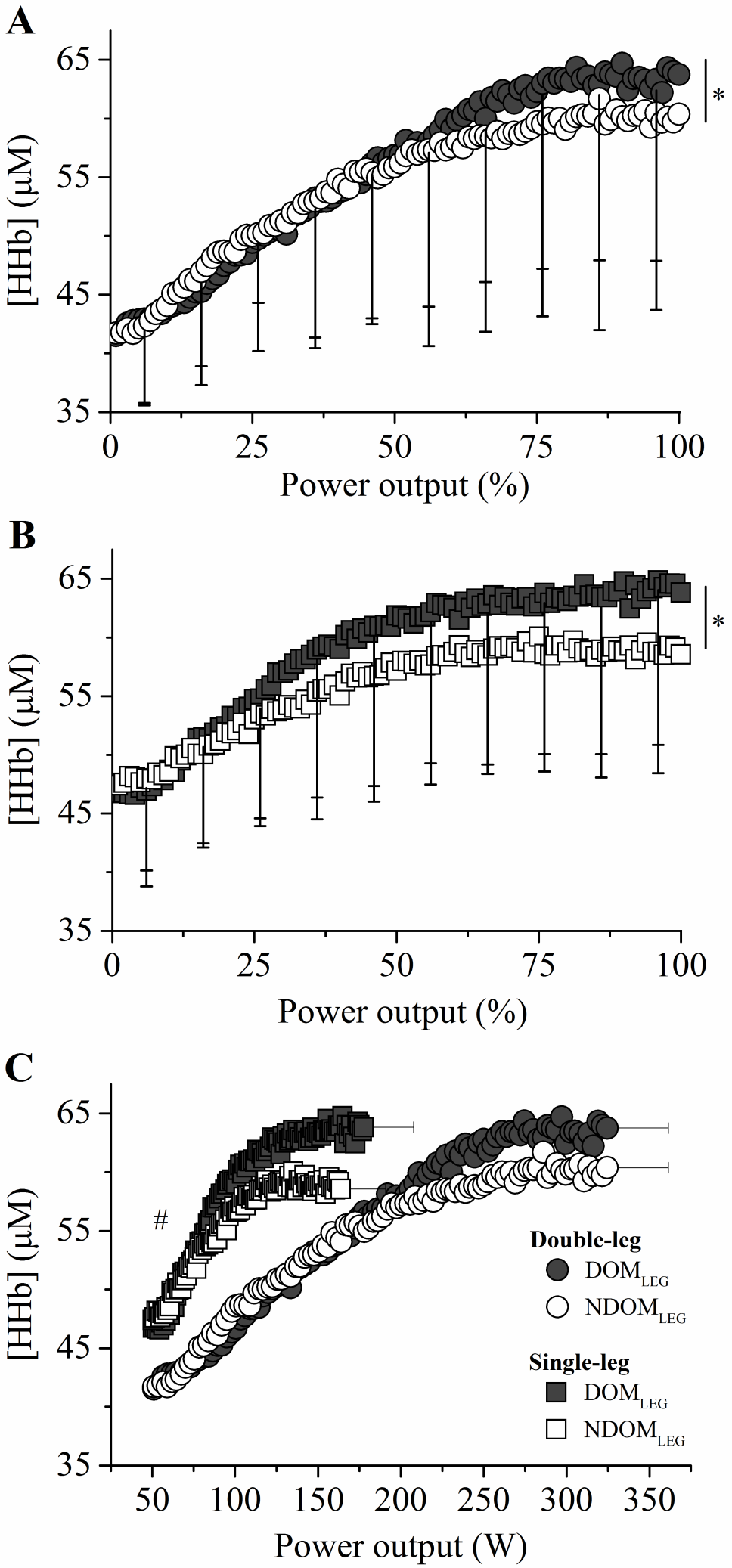
A
[HHb] (μM)
65
55
45
35
0
25
50
75
100
Power output (%)
*
B
[HHb] (μM)
65
55
45
35
0
25
50
75
100
Power output (%)
*
C
[HHb] (μM)
65
55
45
35
#
Double-leg
DOM$_{LEG}$
NDOM$_{LEG}$
Single-leg
DOM$_{LEG}$
NDOM$_{LEG}$
50
100
150
200
250
300
350
Power output (W)

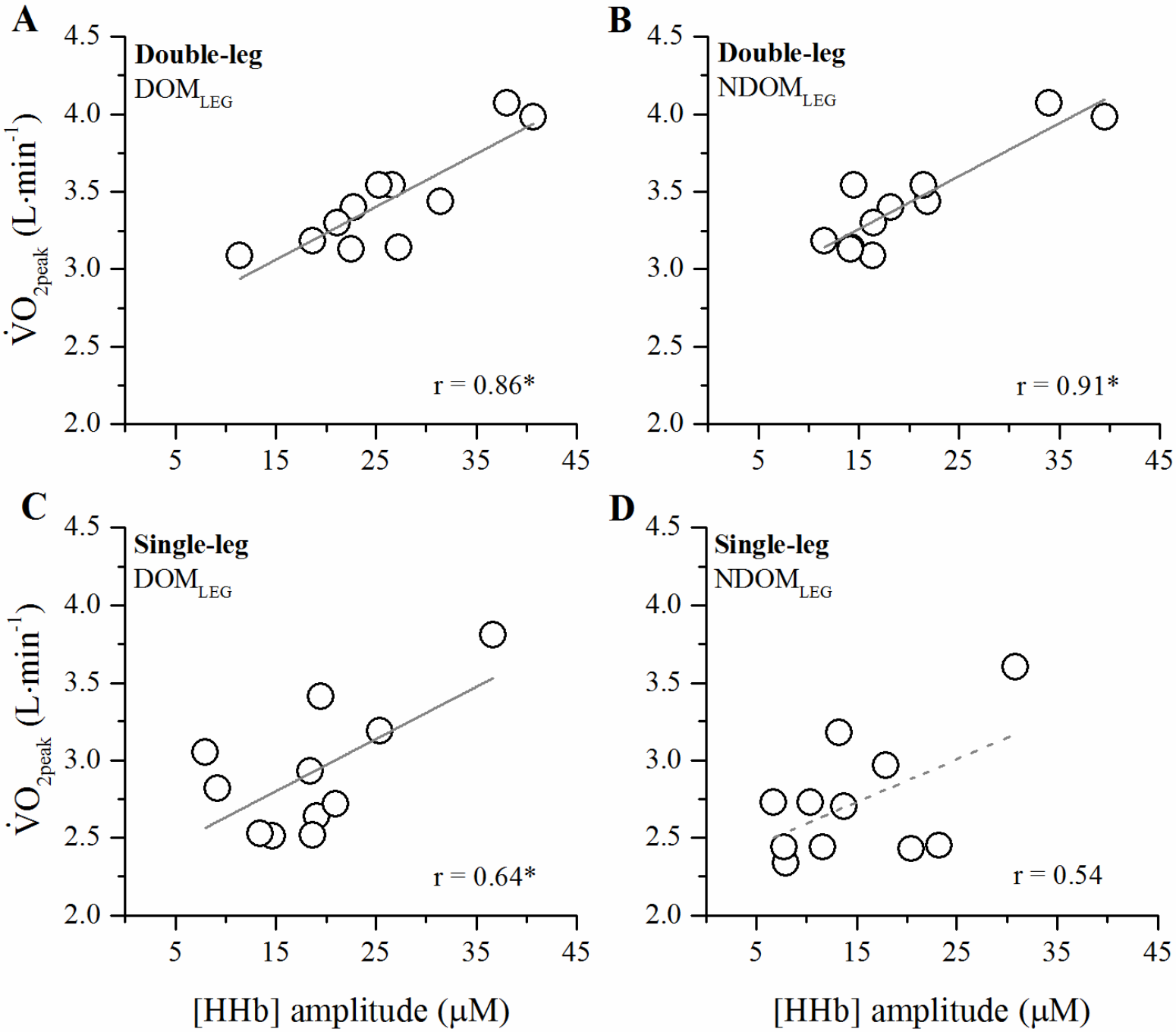
A
Double-leg
DOM$_{LEG}$
r = 0.86*
B
Double-leg
NDOM$_{LEG}$
r = 0.91*
C
Single-leg
DOM$_{LEG}$
r = 0.64*
D
Single-leg
NDOM$_{LEG}$
r = 0.54
$\dot{V}O_{2peak}$ (L·min^{-1})
[HHb] amplitude (μM)
4.5
4.0
3.5
3.0
2.5
2.0
5
15
25
35
45

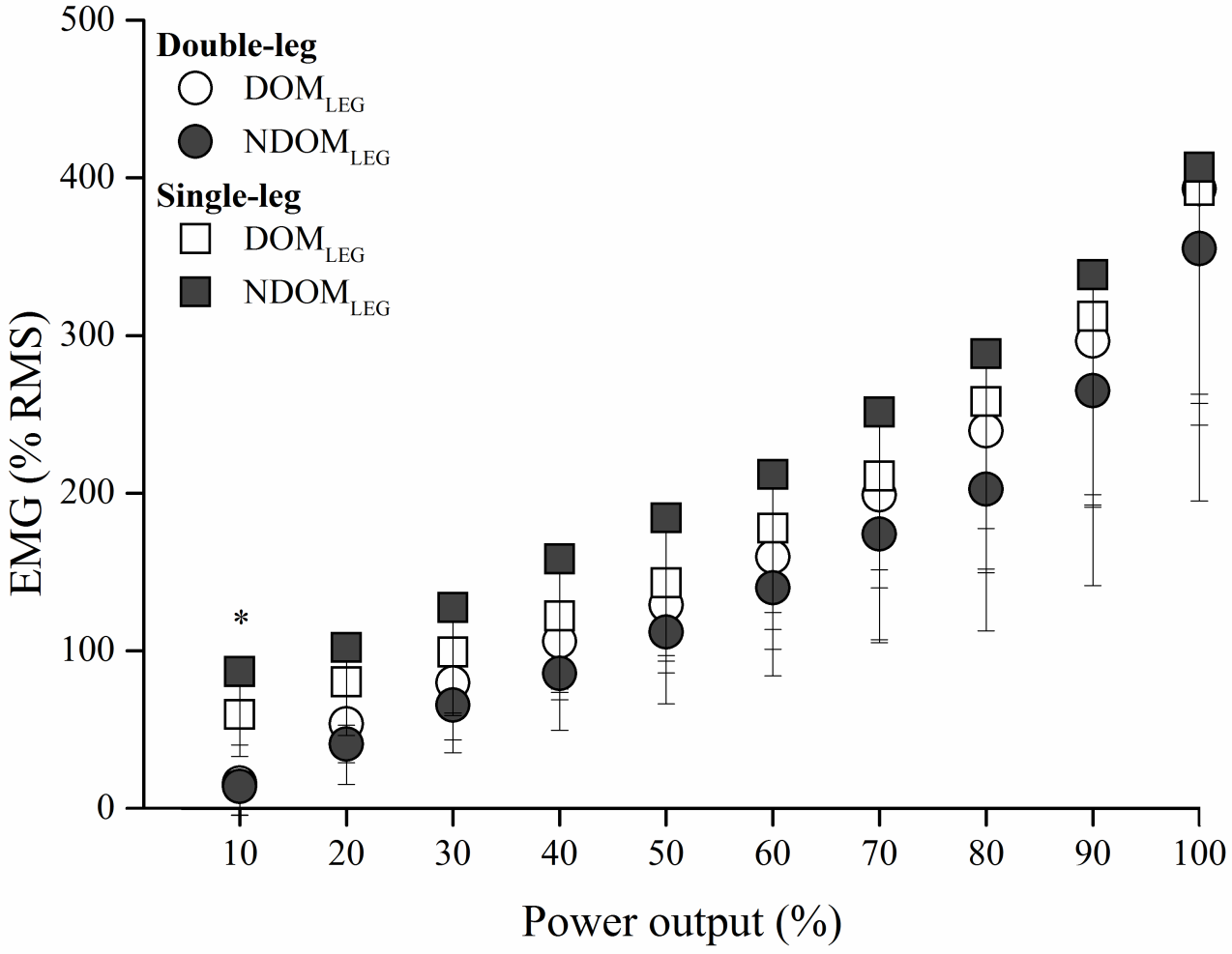
Double-leg
DOM LEG
NDOM LEG
Single-leg
DOM LEG
NDOM LEG
EMG (% RMS)
500
400
300
200
100
0
*
10
20
30
40
50
60
70
80
90
100
Power output (%)

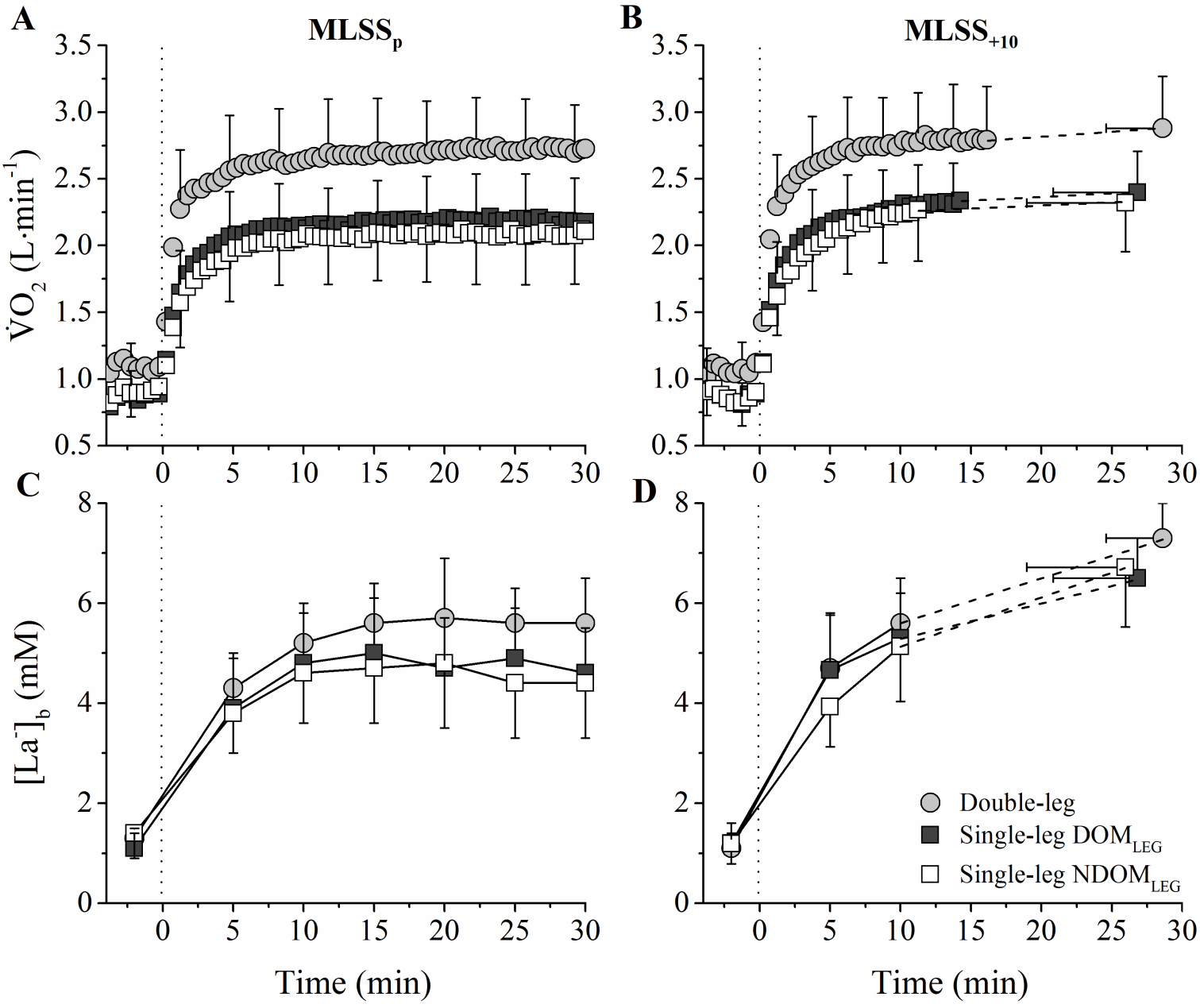
A
MLSSp
B
MLSS+10
C
D
V̇O2 (L·min-1)
[La-]b (mM)
Time (min)
Time (min)
Double-leg
Single-leg DOMLEG
Single-leg NDOMLEG

Table 1. Peak physiological responses during double-leg, and dominant (DOM_{LEG}) and non-dominant ($NDOM_{LEG}$) counterweighted single-leg cycling ramp-exercise.

Exercise mode	Double-leg	Counterweighted single-leg	
		DOM_{LEG}	$NDOM_{LEG}$
PO_{peak} (W)	327±37	179±30 *	165±27 *,#
$\dot{V}O_{2bsln}$ ($L \cdot min^{-1}$)	1.16±0.12	1.14±0.10	1.12±0.14
$\dot{V}O_{2peak}$ ($L \cdot min^{-1}$)	3.43±0.33	2.87±0.42 *	2.70±0.39 *,#
$\dot{V}O_{2peak}$ ($mL \cdot kg^{-1} \cdot min^{-1}$)	45.1±6.1	-	-
G_{ramp} ($mL \cdot W^{-1} \cdot min^{-1}$)	9.2±1.0	-	-
G_1 ($mL \cdot W^{-1} \cdot min^{-1}$)	-	12.1±2.5 §	12.3±2.0 §
G_2 ($mL \cdot W^{-1} \cdot min^{-1}$)	-	17.9±7.3 §	19.4±7.0 §
HR_{max} (bpm)	180±12	164±10 *	165±27 *
$\dot{Q}_{peak}$ ($L \cdot min^{-1}$)	20.7±2.9	19.0±2.3 *	17.8±2.4 *,#
$[La^-]_b$ (mM)	12.4±1.7	8.2±1.6 *	8.0±1.6 *

Data are presented as mean±SD; PO_{peak}: peak power output. $\dot{V}O_{2bsln}$: baseline rate of O_2 uptake at 50 W. $\dot{V}O_{2peak}$: peak rate of O_2 uptake; G_{ramp}: $\Delta\dot{V}O_2/PO$ during double-leg ramp-exercise; G_1 and G_2: $\Delta\dot{V}O_2/PO$ during single-leg ramp-exercise within the first and second portion of the ramp-exercise, respectively; HR_{max}: maximal heart rate. $\dot{Q}_{peak}$: peak cardiac output. $[La^-]_b$: blood lactate concentration immediately after the ramp-exercise.

* Denotes significance from double-leg.

# Denotes significance from DOM_{LEG}.

§ Denotes significance from G_{ramp} of double leg

Table 2. Baseline, amplitude, and slope of increase in the [HHb] signal of the vastus lateralis during double-leg, and dominant (DOM_{LEG}) and non-dominant ($NDOM_{LEG}$) counterweighted single-leg cycling ramp-exercise.

Exercise mode	Double-leg		Counterweighted single-leg	
	DOM_{LEG}	$NDOM_{LEG}$	DOM_{LEG}	$NDOM_{LEG}$
Baseline (μM)	41.2 ±8.6	41.1±9.0	45.9±7.3	46.8±7.3
Amplitude (μM)	26.0±8.4	20.2± 8.8 *	18.5±7.9 *	14.9±7.5 *,#,§
$S1_{(\%PO)}$	0.41±0.22	0.42±0.26	0.43±0.36	0.42±0.36
$S2_{(\%PO)}$	0.00±0.02	0.00±0.02	0.01±0.02	0.01±0.02
$S1_{(W)}$	0.10±0.06	0.10±0.07	0.16±0.06 *	0.18±0.08 #
$S2_{(W)}$	0.00±0.02	0.00±0.02	0.01±0.02	0.01±0.02

Data are presented as mean ± SD. *S*1 and *S*2 are slope 1 and 2 of the [HHb] signal calculated against relative (%PO) and absolute (W) power output.
* Denotes significance from double-leg DOM_{LEG}.
# Denotes significance from double-leg $NDOM_{LEG}$.
§ Denotes significance from counterweighted single-leg DOM_{LEG}.

Table 3. Power output (W) and $\dot{V}O_2$ ($L \cdot min^{-1}$) data at $MLSS_p$ and $MLSS_{+10}$.

Exercise mode	Double-leg		Counterweighted single-leg			
			DOM_{LEG}		$NDOM_{LEG}$	
Condition	$MLSS_p$	$MLSS_{+10}$	$MLSS_p$	$MLSS_{+10}$	$MLSS_p$	$MLSS_{+10}$
Power output (W)	183±31	193±31 *	118±24 #	128±24 *,#	109±23	119±23 *
Power output (% of double-leg)	-	-	65.5±8.8 #	66.4±8.3 *	60.0±8.4	62.1±8.0 *
$\dot{V}O_{2bsln}$	1.11±0.09	1.06±0.16	1.19±0.10	1.14±0.10	1.19±0.12	1.15±0.11
$\dot{V}O_{2end}$ ($L \cdot min^{-1}$)	2.73±0.32	2.87±0.28 *	2.18±0.25 #,§	2.39±0.31 *	2.09±0.29	2.33±0.31 *
$\dot{V}O_{2gain}$ ($ml \cdot min^{-1} \cdot W^{-1}$)	12.3±1.1	12.8±1.6	15.4±3.4 ^	16.6±3.24	15.6±3.3 ^	17.9±3.3
$\dot{V}O_2$ (% of double-leg)	-	-	79.9±7.3 #	87.8±9.3 *	76.5±7.8	85.7±10.1 *

Data are presented as mean±SD. $\dot{V}O_{2bsln}$: baseline rate of O_2 uptake at 50 W; $\dot{V}O_{2end}$: rate of O_2 uptake during the last two minutes of the constant-load trials.
Percent values of power output and $\dot{V}O_2$ are calculated based on the double-leg $MLSS_p$.
* Denotes significance from $MLSS_p$ of same exercise mode.
# Denotes significance from $NDOM_{LEG}$ of same condition.
§ Denotes significance from $NDOM_{LEG}$ of different condition.
^ Denotes significance from double-leg of same condition.